CRYOGENIC PHASED ARRAY FEED

EFFELSBERG PAF EVALUATION JUNE 2018

REVISION : 1.0

RELEASED : 10.7.2018

Author :	
Name	*Stefan Heyminck, Xinping Deng*
Institute	*MPIfR*
Function	*Project manager, Work-package manager*

Approved :		***Date :*** *10.7.2018*
Name	*S. Heyminck*	
Institute	*MPIfR*	
Function	*Project manager*	

Keywords:

Evaluation and commissioning of the warm PAF system at the Effelberg 100m telescope in June 2018

Revision	***Change***	***Pages***	***Date***
Draft	*Released*	*all*	*6.7.2018*
1.0	*Changes and completions*	*all*	*10.7.2018*

TABLE OF CONTENTS

LIST OF ACRONYMS

MPIfR	Max-Planck-Institute for Radioastronomy
CAS	Chinese Academy of Science
FWHP	Full width half power
IRIG-B	Inter range instrumentation group (timecode of subgroup B)
PAF	Phased Array Feed
PSU	Power supply unit
RF	Radio-Frequency
TEC	Thermoelectric cooler
TOS	Telescope operating system (for PAF frontend and backend)

1 INTRODUCTION

The PAF was installed on Monday June 25th 2018. Observing started on the same day at 5pm.

Objectives: According to "PAF Testplan for June 25th – July 2nd", document number cryoPAF PLA 2170-01.

The testing in the testplan reads to be nice and easy. But in reality we have been surprised by a lot of problems, lack of understanding and experience with the receiver system (especially with the new version of the receiver software), and problems in the telescope receiver interplay. In the end we learned a lot but most of the proposed measurements and tests could not be performed as required / planed.

2 PROBLEMS

2.1 HARDWARE PROBLEMS

We detected several hardware problems or problems with the configuration of the hardware.

2.1.1 POWER SUPPLY FOR THE RF POWER CONTROL-MODULE

The power supply of the RF power control-module is a standard connector power supply. The therefore quite heavy 230V connector can create a bad contact or even fall of the socket when driving the telescope in Elevation.

In future we need a more solid approach (e.g. a rack mountable power supply) to increase reliability (System group is already working on this issue). For the moment the power supply was fixed at an extension cord with Duck-tape and zip-ties.

2.1.2 TEC CONTROLLER

The temperature control module did not work correctly after the installation. The control software did not show any currents on the system. The problem could not be fixed in the focus cabin and was all of a sudden gone. Likely: A bad connection to the power supply was responsible for the problem.

In principle we need to reproduce the failure in the lab and then fix it prior to the next observing run. But to do so we need to connect the frontend to the receiver network. This requires fiber-connections from the lab area to the control room. This is maybe not feasible (needs discussion). As an alternative we could ruggedize the power supply and its connections prior to the next installation and if the error pops up again debug it in the antenna.

The regular procedure to verify the functionality of TEC is waiting for about half an hour until the temperature of PAF frontend reaches its turning point (25 °C). If everything works well, a voltage and current output from TEC should be indicated by the software. Since this is a lengthy procedure and the result is not always conclusive we should find a better way to check the TEC

2.1.3 SWITCH LOSES CONFIGURATION

The switch within the GPU cluster sometimes loses its configuration (e.g. after power cycling) and goes back to its default settings. Then the "ageing-time" is too short and the system loses its pre-defined connections at some point during the observations.

Mitigation: Check settings after start-up of the system and on a regular basis during the observing run (e.g. daily at a fixed time). On long term we need an automated approach here:

E.g. editing the ageing time in the default configurations of the switches set them to 1000000s instead of 300s) and secure that the new configuration is used while powering up the system.

Another approach would be to set up the switches from outside with a startup-script.

In addition we need a manual describing how to solve this problem manually and we should have software based checks with user feedback (e.g. via the telescope control system) during operation to indicate data-flow is correct during operation.

2.1.4 GPU NODE PACFIX5 WAS NOT ACCESSIBLE

The pacfix5 computer node was not accessible at the beginning of the observing run. We need a manual describing how to restart the GPU cluster and the internal switches. In addition we have to make sure that the storage system is re-mounted after the restart.

The problem is maybe related with the loss of connections in the switches (see also chapter 2.1.3). This can possible create high network traffic on the GPU-nodes and therefore makes it inaccessible. Tests are ongoing.

2.1.5 AIRFLOW TO THE BACKEND SWITCHES

The air-flow in the GPU-server rack inside the Faraday room towards the switches was insufficient and tended to create a thermal short cut.

The housings of the switches are much shorter than the server housings. For better access of the connectors they are mounted in alignment with the server back-side. The airflow inside the switches is, as within the servers, from their front to back side. To guide the cool air inside the servers the front-side of the rack, where the air enters, is closed and the only openings are the server air-inlets. This is fine for the servers, but bad for the switches which are now isolated from the cool air and suck in the warm air from the back-side via the side of the rack; and hence create a kind of thermal short cut here.

We build from paper and tape an air-well from the rack front-side to the switch air-inlet. Hence we connected the switch air-inlet to the fresh air on the rack front-side without opening an air-bypass to the rack back-side. This works

fine and air outlet temperature of the switches is much lower than before. But this is only a provisional solution. A more solid solution is required in near future.

2.1.6 *ABSOLUTE TIMING*

We detected a time difference of the order of 3.5 seconds between the position data in the meta-data stream, and the voltage value stream (both created / modified within the beam-former). So far it is unclear where the offset is introduced.

The first idea was that this is introduced by the observing itself since we are using the standard pointing and mapping procedures of the telescope. These are scanning modes and not adapted to the PAF. But using a raster type scan in Azimuth via the beam-former weights observing mode (adapted to the PAF and no scanning involved) gave the same time-shift.

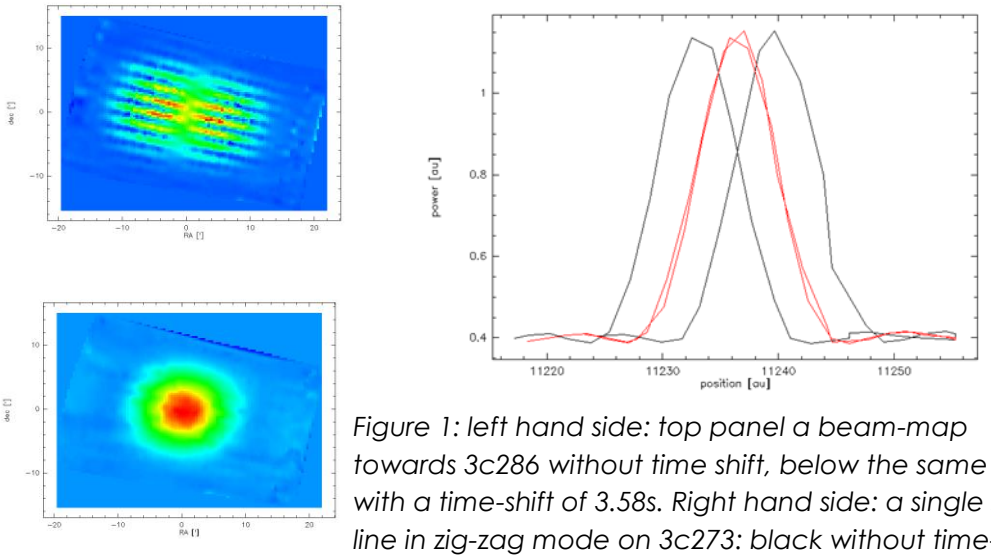

Figure 1: left hand side: top panel a beam-map towards 3c286 without time shift, below the same data with a time-shift of 3.58s. Right hand side: a single scan line in zig-zag mode on 3c273: black without time-shift, red with time shift of 3.11 s.

The telescope is synchronized to the IRIG-B signal and this signal is also directed to the PAF system. Since none of the other receivers has such a problem it is very likely that it is PAF system related.

There are several locations where this can happen:

- The internal timing supply is not synchronized to the telescope,
  - e.g. IRIG-B is not connected or not used.

  ➔ Any time-delay is possible
- The flux calculation pipeline introduces a time-offset.

  ➔ Time delay usually should be in the order of half of the integration time (here 0.9s).

This effect is present and seems to reduce the overall shift by half of the integration time. The calculation will be corrected for the next run.

- The beam-former internal algorithm calculating the meta-data time-stamps is inaccurate / insufficient.
  ➔ Effect is unclear

We need to check the PAF timing system and its synchronization with the telescope prior to the next observing run. In addition we have to get an understanding how time-stamps are processed by the beam-former system. As last action we have to verify that the flux calculation pipeline deals correctly with the time-stamps of the beam-former voltage stream.

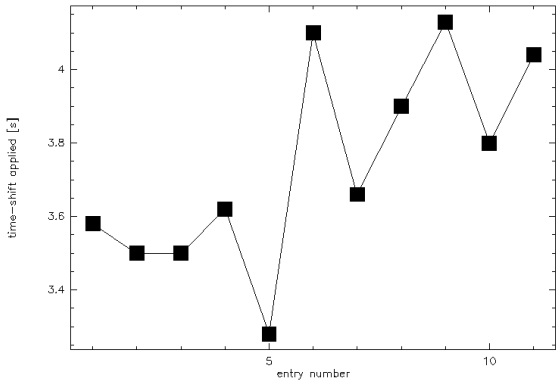

Figure 2: Jitter of the applied time-shift over the observing run. First data taken are plotted on the left and last map on the right.

It seems that the jitter was increasing over time. But since the uncertainty of the shift determination is quite large this may results from the data reduction process itself.

2.2 SOFTWARE PROBLEMS

We had several problems with the PAF control software, but also with the observing system during the run. In addition a valid manual and check lists for the routine tasks (start-up, shut-down, determine beam-former weights, ...) are missing.

2.2.1 *WHICH BEAM-FORMER WEIGHTS ARE USED*

For the upload of the beam-former weights two different GUIs are applicable, but only one of them is (partly?) working. Hence we have seen crazy beam-shapes, unexpected system behavior, and unreliable operations in general.

The uploading of the beam-former weights needs a description in the manual. Important here:

- which GUI has to be used,
- do NOT press the "apply beamweights" button since it kills the data streaming connections,
- where to find the log-file (see below)

The log file shows the filename of the last loaded beam-former weights file. It would be good to automatically display this filename and hence give a feedback for the operator. At least the log file needs to be checked after uploading new beam-former weights. A manual describing these tasks will be provided in future.

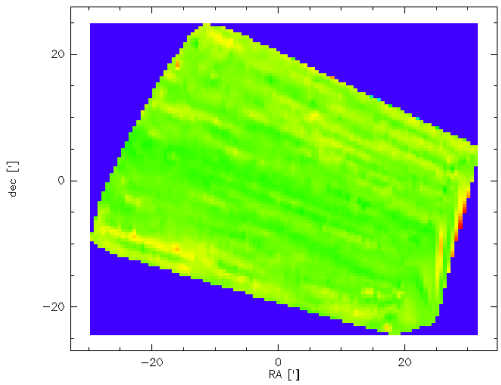

Figure 3: Not an unusual beam-map. Because of unnoticed software failures / operation-mistakes the data recorded is unusable. In this case 3c286 is invisible because beam-former weights were not uploaded correctly.

2.2.2 *Losing reference in beam-forming observation*

We had one time the issue of losing the data of the reference observations of the beam-former observing sequence. This could potentially denote to a problem in the interplay between telescope software and receiver software. The only fix at the moment is to redo the observations.

2.2.3 *Change of the frequency band*

The procedure of how to change the frequency band within the PAF was unclear and therefore not reliably working. So far we can't tell that the procedure derived during the tests is reliable under all circumstances. Hence one needs to check the active frequency band via the spectral response. This is applicable using a script on the TOS computer. Both, the switching procedure and the checking of the spectral response must be described in a

manual for the PAF. In addition a direct user feed-back via a GUI application or even better via the telescope control system would be nice.

2.2.4 *TELESCOPE CONTROL SYSTEM*

In the beginning we had problems with the "new" telescope control Software. The control task crashed regularly. This was fixed by the telescope science support. Later we experienced several times a very slow or crashing VNC for the observing clients. This could be (at least once) solved by using the old queue-manager. The "new one" seems to create a high load on the graphics system. If this is the real reason for the slow, often unusable system is unclear. We need to find out if this is a PAF related issue (maybe because of the insufficient backend and frontend connections) or a more general problem.

If the VNC is slow it usually can be recovered by restarting the VNC server for this particular VNC. Of course the software tasks running there need to be restarted as well.

We had the feeling that connecting with a "wrong" type of VNC client could also cause a slowing down or crashing of the VNC server.

3 BEAM-SHAPE AND POINTING

The measurements of the individual focus curves and their fitting gave us for the center frequency band good data on the beam-size versus frequency (see also chapter 0). The large in focus map to detect side lopes failed during the scan. Hence we do not have a map of the side-lopes. Nevertheless in the line scans the first side-lop is clearly visible and at a descent low level.

In addition we could verify the pointing with the data taken on 3c286.

3.1 BEAM-SHAPE

The beam looks clean and has in the maps a low side lobe level. As mentioned above the large map to make the side lobe visible was incomplete and not usable. The only side lobe impression we got from a cross scan on 3c273. But the side lobe level seems to be higher than the visible side lobe of the maps.

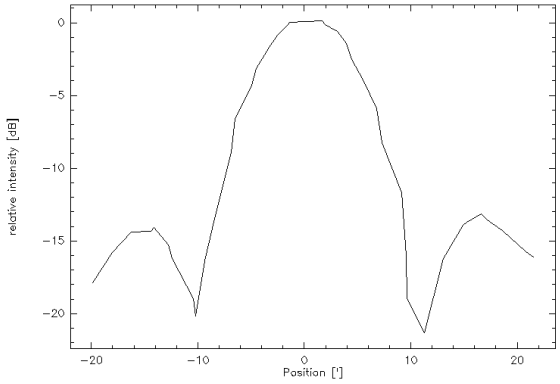

Figure 4: First side-lobes of the main beam are more than 10 dB below the main beam maximum power. Scan was taken on 3c273.

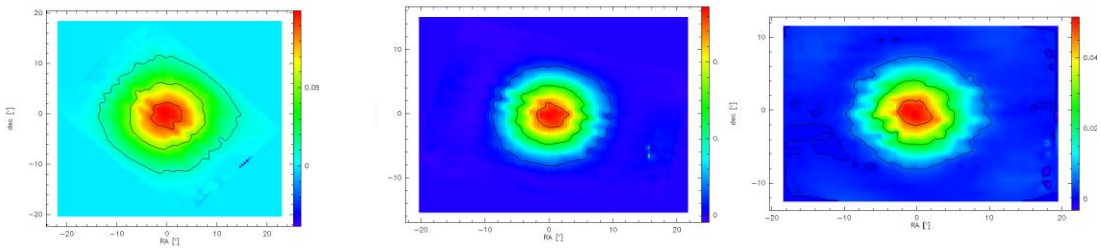

Figure 5: Beam-maps of all three frequency bands (lowest frequency at left hand side). Contours, as far as available are on 90%, 50% 10% and 1% level. A side lobe above 2% as indicated from the cross scan above should be visible in all maps.

The beam is as far as we can tell with the timing uncertainties round and clean. A larger map with better signal to noise is required to trace down the first side lobe correctly.

3.2 BEAM SIZE

Beam sizes are fitted along with the data for the focus. We could derive the beam-sizes nearly over the full frequency range. Due to the beam-forming system, the beam size of each 1 MHz wide frequency channel is in principle independent. The algorithm used for the beamforming is so far not understood by us (we need further investigations and more time here). Nevertheless, the strong frequency dependence of the beam-size was unexpected.

The beam-size of the formed beam changes relative to the diffraction limit with frequency (all measurements taken on 3c286). At the low frequency end it is nearly 1.4 times the diffraction limit, and hence we do not use the full dish her. At the high frequency end it is about 1.1 times the limit. A well matched horn antenna based receiver usually has a beam about 1.1to 1.2 times larger than the diffraction limit.

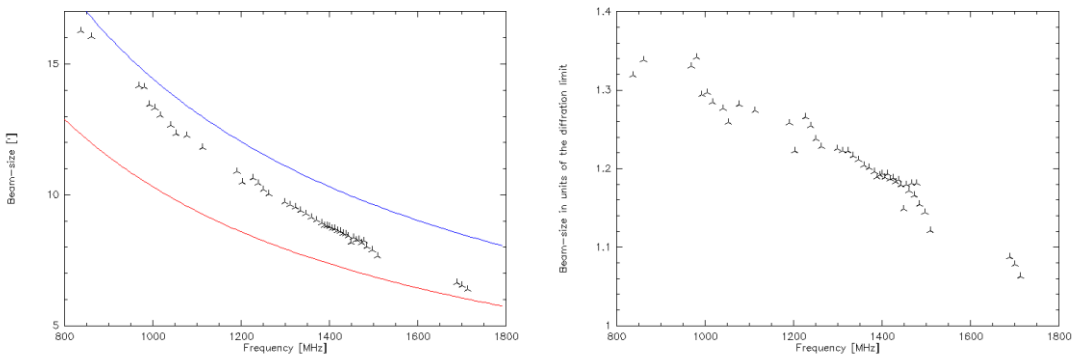

Figure 6: Fitted beam-size (black triangles) versus frequency. The red curve denotes the diffraction limit of a 100m dish and the blue curve is at 1.4 time of this value. The right hand side figure shows the beam-sizes in units of the diffraction limited beam. We fitted the beam-maps using 12 MHz wide frequency chunks for all three frequency bands of the PAF. But the high and the low band had a lot of RFI within. Therefore the data-quality especially towards the lower and the higher end of the plot is limited. In the area around 1400 MHz the mid and high band overlap. Both data sets are in good agreement here.

The reason for this behavior is unclear to us. It could result from the interplay between maximum signal to noise beam-former and the frequency dependent illumination function of the individual antenna. Also RFI could play a role here.

3.3 POINTING

Along with the data fitting we could also derive the pointing of the individual frequency channels in respect to each other. In addition we got several observations of the same object (3c286) on its trajectory over the Effelsberg sky.

In the last map we took during this run (on June 30th) we detected a pointing offset. So far we never checked the position, but here it was done. The pointing was off by about 2', more than 20% of the FWHM beam-size.

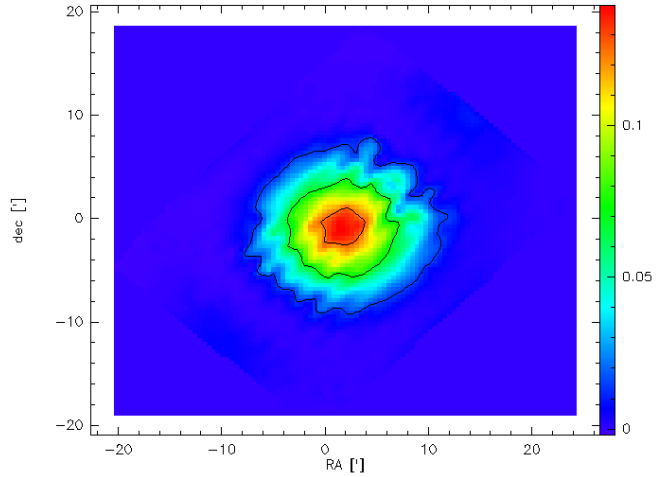

Figure 7: Map of 3C286 in the late morning directly after it came up. The offset of 1.7' in RA and -1' in dec is visible by eye already.

After we detected the offset we looked at all other offsets in the data. They have been fitted together with beam-sizes and signal strength for the focus measurements. One can see a clear trend of the pointing offset with the time of the day. This means the offset changes with the sky rotation and therefore this denotes that the main beam is formed of center of the telescope focal plane.

Why this is the case we do not know at the moment. One can speculate:

- beam-former uses wrong epoch for its calculations;
- signal to noise beam-former weight determination algorithm is influenced by RFI;
- pointing constants used for the PAF within the telescope system are wrong;
- using the scanning modes introduce an position error (scanning pattern rotates with the source)
- ….

For all of the above points it is unclear if they can explain the effect. Nevertheless a pointing offset of up to 2' will influence the astronomical data and must be taken out.

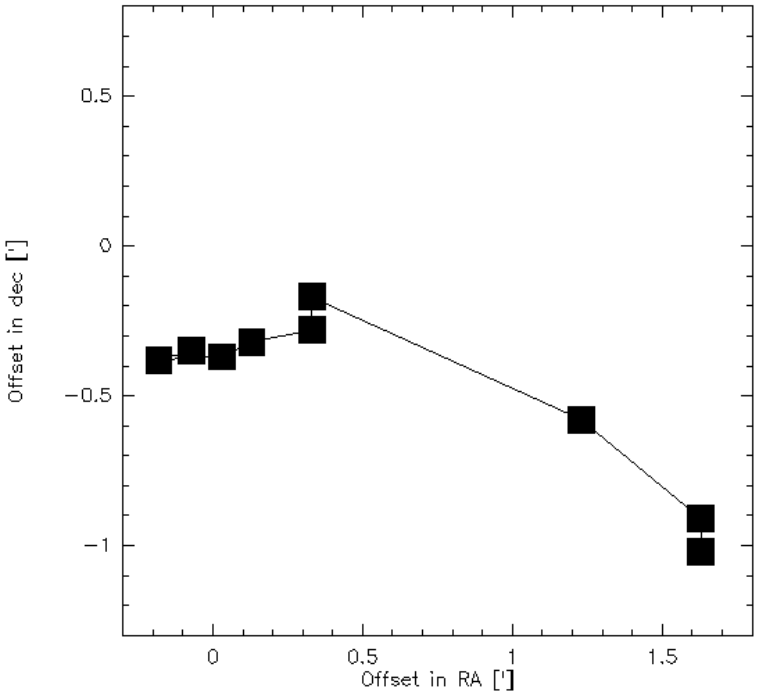

Figure 8: Offsets in the position of 3c286. The positions are connected in the order of the time of the day, starting at the right hand side with large RA-offsets around 13:30 and stopping at the left end with an RA offset of zero around 20:50.

4 FOCUS CURVE

We tried to re-do focus curves with two different approaches (just changing focus without re-do measurements for new beam-former weights, and re-measure and re-calculate the beam-former weights after changing z-focus). In the original planning we also wanted to check the off-axis beams. The last was dropped due to the time limitations we faced with all the technical problems. In addition we had to reduce the number of z-positions for the boresight beam.

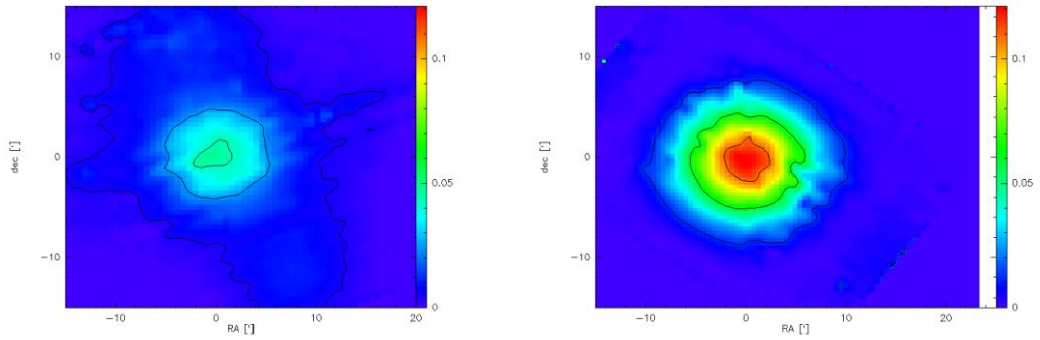

Figure 9: Comparison of the beam without new beam-former weights (left hand side) 164mm out of the nominal focus and with new beam-former weights (right hand side) 200mm off focus. Intensity scale was held fix on both plots; contour levels are at 90%, 50%, and 10% of the maximum intensity.

We measured a beam-map at each focus point and derived beam-size and amplitude over the RF-band and as an average value out of a RFI free frequency band.

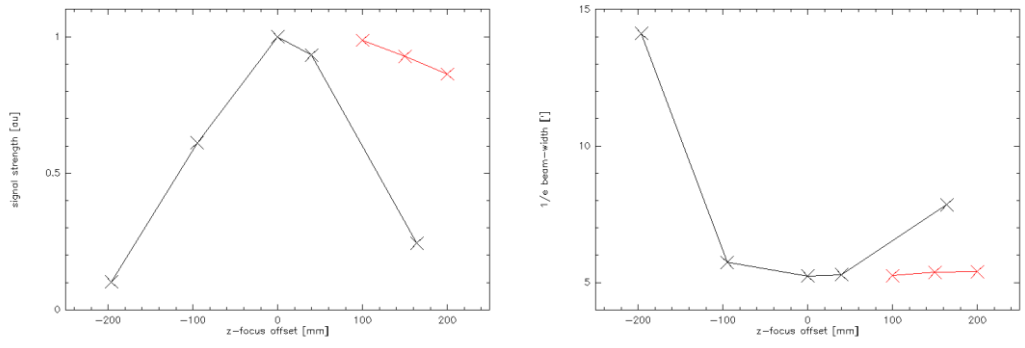

Figure 10: Derived focus curves: Left hand side from averaged signal amplitude and Right hand side from averaged beam-width. Average was taken from frequency channels 180 to 300. The black curve denotes the values without re-measuring and re-calculating beam-former weights after changing Z-focus; the red curves show the values when new beam-former weights were calculated after the focus change.

Our measurements show the expected behavior: without new beam-former weights the focus behaves as any usual receiver (black curves in figure

above). In contrast, the red curves show that the beam-forming measurements are self-focusing over a wide Z-focus range. If this is true also for off-axis beams in the same extend needs to be proven in future.

The system temperature for the three of focus curves with re-measured and re-calculated beam-weights increases proportional with roughly 1 over signal strength. Hence the 100mm defocused system has nearly the same system temperature while the one of the 200mm defocused system is increased by about 10%.

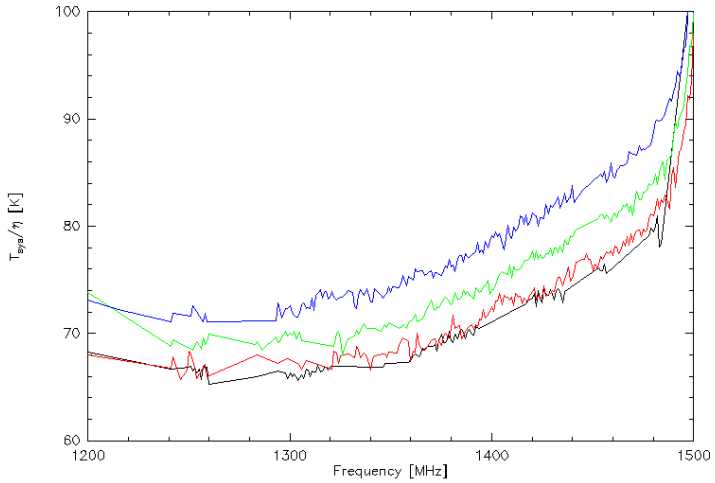

Figure 11: Tsys/η for the focus offsets at which the beam-former weights have been re-measured: black – in focus, red – 100mm off focus, green – 150mm off focus, and blue – 200mm off focus. RFI was removed by hand from the data.

If beam-former weights are re-measured and updated regularly, taking a focus curve and re-focusing the receiver is not necessary during usual operation. In what intervals beam-weights need to be re-calculated and updated is still (a bit) unclear. The system seems to be stable over days, hence once per day should definitely be sufficient from what we can tell so far.

5 CONCLUSIONS

We learned much about the PAF system and its operations. We could derive procedures for the handling and detected some hardware short-comings. In addition we learned a bit about the intrinsic characteristics of a PAF system. The last point was the main objective of the test-plan but could only be touched slightly since the test time was occupied mostly by solving the various problems operating the system.

Therefore from our perspective the To-Do list for the next run must start with writing up a manual including all necessary PAF operating procedures. This will reduce dead times and overheads already massively and in addition secure the data quality.

In parallel we need to fix all the hardware hick ups found and find the reason for the time delay in between telescope position meta-data stream and beam-former voltage stream. At least we need to understand the effect and being able to denote the delay-time accurately prior to the next observing run. Also we need to do a pointing session at the beginning of the next observing run. We need to trace down the reason for the quite large pointing offsets we detected.

As a second step we should start to design an operator GUI which gives a quick and easy feedback about the actual instrument status. On longer term we should establish a connection to the telescope drive system to make this information available to the operator / astronomer directly.

As a last step we suggest to perform a receiver system check every so often between / during observations (e.g. every 3 hours, after changing frequency bands, after loading different beam-former weights, …). This can be done on several ways. One option is to write a backend interface towards the telescope fits-writer for flux data. This enables to check beam-quality on known point sources using the standard measurement procedures (Pointing, or mapping) and therewith the operational status of the receiver directly. Another possibility is to observe a known Pulsar as reference. Also for such a measurement we suggest to set up an automated approach (press one knob and get the result directly displayed – best via the online plotter of the telescope control system) to increase the acceptance for such a test by the observers / operators.

Especially with the above mentioned pointing inaccuracies of up to 2' one needs to check the pointing on a regular basis on a source close to the observing target (at least as long as the reason for this is unclear).